Determining the Bohm criterion in plasmas with two ion species

S. D. Baalrud[a] and C. C. Hegna
Department of Engineering Physics, University of Wisconsin–Madison, 1500 Engineering Drive, Madison, Wisconsin 53706-1609, USA

(Received 28 November 2010; accepted 25 January 2011; published online 28 February 2011)

A model that uniquely determines the flow speed of each ion species at the sheath edge of two ion species plasmas is developed. In this analysis, ion-ion two-stream instabilities can play an important role because they significantly enhance the friction between ion species. Two-stream instabilities arise when the difference in flow speeds between the ion species exceeds a critical value: $V_1 - V_2 \equiv \Delta V \geq \Delta V_c$. The resultant instability-enhanced friction rapidly becomes so strong that ΔV cannot significantly exceed ΔV_c. Using the condition provided by $\Delta V = \Delta V_c$ and the generalized Bohm criterion, the speed of each ion species is uniquely determined as it leaves a quasineutral plasma and enters a sheath. Previous work [S. D. Baalrud *et al.*, Phys. Rev. Lett. **103**, 205002 (2009)] considered the cold ion limit ($T_i \to 0$), in which case $\Delta V_c \to 0$ and each ion species obtains a common "system" sound speed at the sheath edge. Finite ion temperatures are accounted for in this work. The result is that ΔV_c depends on the density and thermal speed of each ion species; ΔV_c has a minimum when the density ratio of the two ion species is near one, and becomes larger as the density ratio deviates from unity. As ΔV_c increases, the speed of each ion species approaches its individual sound speed at the sheath edge. © *2011 American Institute of Physics*.
[doi:10.1063/1.3555533]

I. INTRODUCTION

In 1949 Bohm showed that ions must have a supersonic flow speed, $V_i \geq \sqrt{T_e/M_i}$, as they exit a quasineutral plasma and enter a non-neutral sheath.[1] It has since been shown theoretically[2] and experimentally[3] that equality typically holds in this relationship. The Bohm criterion has become one of the most famous results in plasma physics because knowing the speed at which ions leave a plasma is important for determining how a plasma interacts with a material boundary. For example, it facilitates calculation of the current, particle and heat flux transferred to a boundary. It is used in nearly all areas of plasma physics including materials processing,[4] fusion,[5] space,[6] and diagnostics.[7] It is also used as a boundary condition in many numerical simulations of plasmas.[8]

Although the Bohm criterion has been tremendously successful at describing the velocity of ions at the sheath edge of single ion species plasmas, it becomes ambiguous when generalized to plasmas with multiple ion species. For the same type of plasma that Bohm considered (one with singly charged monoenergetic ions with velocity $\mathbf{V}_i$ and Boltzmann electrons with temperature T_e) but allowing for N ion species, the Bohm criterion becomes[9–11]

$$\sum_i^N \left. \frac{n_i}{n_e} \frac{c_{s,i}^2}{V_i^2} \right|_{z=0} \leq 1, \tag{1}$$

in which i label the different ion species, $z=0$ denotes the sheath edge, and $c_{s,i} \equiv \sqrt{T_e/M_i}$ is the individual species sound speed of the ith ion species. Equation (1) has also been generalized to account for arbitrary ion and electron distribution functions,[12] including finite ion temperature corrections, but these are typically small as long as $T_e \gg T_i$.[13] We concentrate on the $T_e \gg T_i$ regime in this work. For $N>1$, Eq. (1) does not uniquely determine the speed of each ion species as it leaves a plasma if equality is assumed. In particular, for $N=2$ Eq. (1) becomes

$$\frac{n_1}{n_e}\frac{c_{s,1}^2}{V_1^2} + \frac{n_2}{n_e}\frac{c_{s,2}^2}{V_2^2} = 1. \tag{2}$$

Equation (2) is a single equation in the two unknowns V_1 and V_2. Thus, a second constraint is required in order to uniquely determine the speed of each ion species as it leaves a quasineutral plasma.

The conventional solution of Eq. (1) put forth in previous theoretical literature is that each ion species obtains its individual sound speed at the sheath edge: $V_i = c_{s,i} \equiv \sqrt{T_e/M_i}$. This solution can be obtained as follows. The one-dimensional steady state fluid momentum equation for each ion species is

$$M_i n_i V_i \frac{dV_i}{dz} = n_i e E - \frac{dp_i}{dz} - \frac{d\Pi_{zz,i}}{dz} + R_i. \tag{3}$$

Here R_i is a frictional force density, which is typically neglected. Assuming that $T_e \gg T_i$, the pressure and stress gradient terms in Eq. (3) can also be neglected since the expectation is that $V_i \sim \mathcal{O}(\sqrt{T_e/M_i})$ near the sheath edge. With these assumptions, Eq. (3) reduces to

$$\frac{M_i}{2}\frac{dV_i^2}{dz} = -e\frac{d\phi}{dz}. \tag{4}$$

Integrating Eq. (4) with respect to z from the bulk plasma (where it is assumed that $V_i=0$) to the sheath edge gives a

[a]Present address: Center for Integrated Computation and Analysis of Reconnection and Turbulence, University of New Hampshire, Durham, New Hampshire 03824.

simple conservation of energy relation: $V_i=\sqrt{2e|\phi_{ps}|/M_i}$. Here ϕ_{ps} is the potential drop between the presheath and bulk plasma. Putting this into the Bohm criterion of Eq. (1), gives the result $e|\phi_{ps}|=T_e/2$. Thus, the individual sound speed solution is obtained: $V_i=\sqrt{2e|\phi_{ps}|/M_i}=c_{s,i}$. More detailed theoretical and numerical studies have been provided by Franklin.[14–18] These have shown that ion-neutral drag and ionization sources in the presheath can cause some deviation from the individual sound speed solution. However, for common plasma parameters these deviations tend to be small and the individual sound speed solution is a robust prediction of the model equations. Large deviations from the individual sound speed solution are predicted only when the ion-neutral collision cross section is much larger for one ion species than the other.

Theoretical literature has supported the individual sound speed solution since the mid 1990s, but this prediction was not tested experimentally until nearly a decade later. These experiments found a surprising result: the speed of each ion species was measured to be much closer to a common "system" sound speed

$$c_s \equiv \sqrt{\sum_i \frac{n_i}{n_e} c_{s,i}^2} \tag{5}$$

than the individual sound speeds $c_{s,i}$. Most of these experiments employed the laser-induced fluorescence (LIF) technique to directly measure the speed of each ion species as it traversed the presheath and entered the sheath.[19–24] They concentrated on plasmas with two species of positive ions that are both much colder than electrons ($T_i \ll T_e$), a situation in which Eq. (2) gives the appropriate Bohm criterion. The system sound speed solution can be obtained from Eq. (2) if it is assumed that each ion has the same speed: $V_1=V_2$.

Additional experimental evidence for the common sound speed solution has been provided using a combination of electrostatic probes and ion-acoustic waves[25,26] to measure the ion speeds in the plasma-boundary transition region. Oksuz *et al.* have measured the ion-acoustic wave speed at the sheath edge to be twice what it is in the bulk plasma in a two ion species plasma.[26] Taking this observation as an ansatz, Lee *et al.* have shown that it implies each ion species enters the sheath at the common system sound speed.[27] However, no physical mechanism was suggested by which this solution is established, or to explain why the ion-acoustic wave speed doubles.

The fact that experiments have measured the individual ion flow speeds to be much closer to one another than the theoretical models predict suggests that ion-ion friction between the species might be important. If one calculates this from Coulomb interactions in a stable plasma (see Sec. II A) it turns out to be weak for the low-temperature plasma parameters of the experiments. However, it has recently been shown that ion-ion two-stream instabilities can dramatically enhance the friction between ion species.[28] Two-stream instabilities are excited when the difference in flow speeds between ion species exceeds a critical value: $V_1-V_2=\Delta V > \Delta V_c$. This critical speed is characteristic of the ion thermal speed: $\Delta V_c \sim \mathcal{O}(v_{Ti})$. Whenever two-stream instabilities are present, the collisional friction rapidly (within several Debye lengths) becomes so large that it dominates the momentum balance equation and quickly reduces ΔV back to the instability threshold ΔV_c. The creates a very stiff system whereby ΔV effectively cannot exceed ΔV_c. Taking $V_1-V_2=\Delta V_c$ and the Bohm criterion of Eq. (2) as another constraint, one can uniquely determine the flow speed of each ion species as it leaves a plasma.[28] In the limit of cold ion temperatures $\Delta V_c \to 0$, and the common system sound speed solution is obtained.

Ion-ion two-stream instabilities have been measured in the presheath of two ion species plasmas.[20,21] These references show measurements of broad-band noise (significantly above the thermal level) in the megahertz frequency range near the plasma boundaries in Ar–He plasma. They also show that the instability is strongest when the relative concentration of each ion species is similar, and that the instabilities become much weaker when the concentration of one species is much more, or less, than the other. All of these results are consistent with ion-ion two-stream instabilities. Despite these measurements, two-stream instabilities were not thought to play an important role in the presheath due to the small amplitude of the fluctuations.[21,29]

In the following section, we provide a detailed calculation of the ion-ion collisional friction force in a presheath. The stable plasma contribution to this friction is calculated explicitly from the Landau collision operator[30] and is shown to be negligible for the plasma parameters of previous experiments. The instability-enhanced contribution is calculated by first assuming a cold ion model for the two-stream instabilities, in which case $\Delta V_c \to 0$. In Sec. III, a kinetic theory for ΔV_c is developed that includes the stabilizing effects of finite ion temperatures. The result shows that ΔV_c depends on the density, mass and temperature ratio of the ion species. Section IV shows how instability-enhanced collisional friction can be used along with Eq. (2) to uniquely determine the speed of each ion species as it leaves a quasineutral plasma. Theoretical predictions are also compared with a recent LIF experiment conducted in Ar–Xe plasma.[29] Here the density ratio n_1/n_2 is varied and the theoretical prediction is that the ion flow speeds range from individual sound speeds (for large or small n_1/n_2) to near a common system sound speed (for $n_1/n_2 \approx 1$). The theoretical predictions are shown to agree well with the measurements. A summary of the results and suggestions for future experimental tests of the theory are given in Sec. V.

II. ION-ION COLLISIONAL FRICTION IN THE PRESHEATH

Friction is a collisional effect that can be calculated from the collision operator of the plasma kinetic equation $\partial f_s/\partial t + \mathbf{v}\cdot\nabla f_s + (q_s/m_s)\mathbf{E}\cdot\nabla_{\mathbf{v}} f_s = C(f_s)$. Here s denotes the particular species of interest and it is assumed that the plasma is unmagnetized. The total collision operator for species s consists of the sum of component collision operators describing collisions of species s with each species s', including $s=s'$: $C(f_s)=\Sigma_{s'} C(f_s,f_{s'})$. The component collision operators have the Landau form:[30] $C(f_s,f_{s'})=-\nabla_{\mathbf{v}}\cdot\mathbf{J}_v^{s-s'}$ where

$$\mathbf{J}_v^{s-s'} \equiv \int d^3v' \mathcal{Q}^{s-s'} \cdot \left(\frac{f_s}{m_{s'}} \frac{\partial f_{s'}}{\partial \mathbf{v}'} - \frac{f_{s'}}{m_s} \frac{\partial f_s}{\partial \mathbf{v}} \right), \tag{6}$$

and $\mathcal{Q}^{s-s'}$ is a tensor kernel. Lenard[31] and Balescu[32] have shown that in a stable plasma $\mathcal{Q}^{s-s'} = \mathcal{Q}_{\mathrm{LB}}^{s-s'}$ where

$$\mathcal{Q}_{\mathrm{LB}}^{s-s'} = \frac{2q_s^2 q_{s'}^2}{m_s} \int d^3k \frac{\mathbf{kk}}{k^4} \frac{\delta[\mathbf{k} \cdot (\mathbf{v} - \mathbf{v}')]}{|\hat{\varepsilon}(\mathbf{k}, \mathbf{k} \cdot \mathbf{v})|^2}. \tag{7}$$

Here

$$\hat{\varepsilon}(\mathbf{k}, \omega) \equiv 1 + \sum_s \frac{4\pi q_s^2}{k^2 m_s} \int d^3v \frac{\mathbf{k} \cdot \partial f_s / \partial \mathbf{v}}{\omega - \mathbf{k} \cdot \mathbf{v}} \tag{8}$$

is the plasma dielectric function for electrostatic fluctuations in an unmagnetized plasma.

Recently, we generalized Lenard–Balescu theory to also account for collisions in unmagnetized plasmas with electrostatic instabilities.[33,34] For an unstable plasma, the collisional kernel is the sum of the stable plasma (Lenard–Balescu) term and an instability-enhanced collision term: $\mathcal{Q}^{s-s'} = \mathcal{Q}_{\mathrm{LB}}^{s-s'} + \mathcal{Q}_{\mathrm{IE}}^{s-s'}$. The instability-enhanced collisional kernel is[33,34]

$$\mathcal{Q}_{\mathrm{IE}}^{s-s'} = \frac{2q_s^2 q_{s'}^2}{m_s} \int d^3k \frac{\mathbf{kk}}{k^4} \sum_j \frac{\gamma_j}{(\omega_{R,j} - \mathbf{k} \cdot \mathbf{v})^2 + \gamma_j^2} \times \frac{\exp(2\gamma_j t)}{[(\omega_{R,j} - \mathbf{k} \cdot \mathbf{v}')^2 + \gamma_j^2] |\partial \hat{\varepsilon}(\mathbf{k}, \omega) / \partial \omega|_{\omega_j}^2}, \tag{9}$$

in which $\omega_{R,j}$ is the real part of the angular frequency and γ_j the imaginary part of the angular frequency of the jth unstable mode. Time in Eq. (9) is calculated in the rest frame of the unstable mode.

The Bohm criterion is a condition related to the fluid flow speed of ions at the sheath edge. The fluid continuity

$$\frac{\partial n_s}{\partial t} + \frac{\partial}{\partial \mathbf{x}} \cdot (n_s \mathbf{V}_s) = 0, \tag{10}$$

and momentum

$$m_s n_s \left(\frac{\partial \mathbf{V}_s}{\partial t} + \mathbf{V}_s \cdot \frac{\partial \mathbf{V}_s}{\partial \mathbf{x}} \right) = n_s q_s \mathbf{E} - \frac{\partial p_s}{\partial \mathbf{x}} - \frac{\partial}{\partial \mathbf{x}} \cdot \Pi_s + \mathbf{R}_s \tag{11}$$

equations can be derived from the plasma kinetic equation by taking the density moment ($\int d^3v \ldots$) and the momentum moment ($\int d^3v m_s \mathbf{v} \ldots$), respectively. The following fluid flow variables are defined in terms of velocity-space moments of the distribution functions: density $n_s \equiv \int_{-\infty}^{\infty} d^3v f_s$, fluid flow velocity $\mathbf{V}_s \equiv n_s^{-1} \int_{-\infty}^{\infty} d^3v \mathbf{v} f_s$, scalar pressure $p_s \equiv \int_{-\infty}^{\infty} d^3v m_s v_r^2 f_s / 3 = n_s T_s$, stress tensor $\Pi_s \equiv \int_{-\infty}^{\infty} d^3v m_s (\mathbf{v}_r \mathbf{v}_r - v_r^2 \mathcal{I}/3) f_s$, temperature $T_s \equiv n_s^{-1} \int_{-\infty}^{\infty} d^3v m_s v_r^2 f_s / 3 = m_s v_{Ts}^2 / 2$ and frictional force density $\mathbf{R}_s \equiv \int_{-\infty}^{\infty} d^3v m_s \mathbf{v} C(f_s)$. Here $\mathbf{v}_r \equiv \mathbf{v} - \mathbf{V}_s$ is a flow-shifted velocity variable. The Bohm criterion of Eq. (1) can be derived using Eqs. (10) and (11) and Poisson's equation.[9–11] Although friction does not typically contribute to the Bohm criterion, we will show that it can be important for determining the flow speed of individual ion species throughout the presheath.

Since the collision operator is the sum of the Lenard–Balescu term and the instability-enhanced term $C(f_s) = C_{\mathrm{LB}}(f_s) + C_{\mathrm{IE}}(f_s)$, the collisional friction can be written as the sum of the two contributions: $\mathbf{R}_s = \mathbf{R}_{\mathrm{LB},s} + \mathbf{R}_{\mathrm{IE},s}$. Noting that the total collision operator can be written in terms of component collision operators $C(f_s) = \Sigma_{s'} C(f_s, f_{s'})$, the collisional friction can also be written in terms of component contributions $\mathbf{R}_s = \Sigma_{s'} \mathbf{R}^{s-s'} = \Sigma_{s'} (\mathbf{R}_{\mathrm{LB}}^{s-s'} + \mathbf{R}_{\mathrm{IE}}^{s-s'})$. Another property that we will utilize is that the frictional force between individual species is equal and opposite

$$\mathbf{R}^{s-s'} = -\mathbf{R}^{s'-s}. \tag{12}$$

Thus, the friction force will slow one ion species and accelerate the other. This is a direct consequence of the property of conservation of momentum between individual species

$$\int d^3v m_s \mathbf{v} C(f_s, f_{s'}) + \int d^3v m_{s'} \mathbf{v} C(f_{s'}, f_s) = 0. \tag{13}$$

A proof that Eq. (13) is satisfied for both the Lenard–Balescu and instability-enhanced terms is given in Ref. 34.

We are interested in calculating $\mathbf{R}^{s-s'}$, where s and s' label the two ion species. We will assume that each species has a flow-shifted Maxwellian distribution function of the form

$$f_s(\mathbf{v}) = \frac{n_s}{\pi^{3/2} v_{Ts}^3} \exp\left[-\frac{(\mathbf{v} - \mathbf{V}_s)^2}{v_{Ts}^2} \right]. \tag{14}$$

In this case, the friction force density on species s from s' reduces to

$$\mathbf{R}^{s-s'} = -m_s \int d^3v \int d^3v' f_s(\mathbf{v}) f_{s'}(\mathbf{v}') \mathcal{Q}^{s-s'} \cdot \left(\frac{\mathbf{v}' - \mathbf{V}_{s'}}{T_{s'}} - \frac{\mathbf{v} - \mathbf{V}_s}{T_s} \right). \tag{15}$$

In the following two sections, we calculate the stable plasma contribution $\mathbf{R}_{\mathrm{LB}}^{s-s'}$ and the instability-enhanced contribution, $\mathbf{R}_{\mathrm{IE}}^{s-s'}$, to Eq. (15). When applying the calculations to a specific example plasma, the plasma parameters of a particularly well diagnosed experiment from the literature[24,29] will be applied: Ar^+ and Xe^+ ions with $T_e \approx 0.7$ eV, $T_i \approx 0.025$ eV (room temperature) and a neutral pressure $\lesssim 1$ mTorr.

A. Stable plasma contribution

For the characteristic $\mathbf{v}$ in Eq. (15), the dielectric function is approximately adiabatic $\hat{\varepsilon}(\mathbf{k}, \mathbf{k} \cdot \mathbf{v}) \approx 1 + k^{-2} \lambda_{De}^{-2}$. In this case, $\mathcal{Q}_{\mathrm{LB}}^{s-s'}$ reduces to the Landau collisional kernel[30]

$$\mathcal{Q}_{\mathrm{LB}}^{s-s'} = \frac{2\pi q_s^2 q_{s'}^2}{m_s} \frac{u^2 \mathcal{I} - \mathbf{uu}}{u^3} \ln \Lambda, \tag{16}$$

in which $\mathbf{u} \equiv \mathbf{v} - \mathbf{v}'$ and $\Lambda \approx 12\pi n_e \lambda_{De}^3$. In Appendix A it is shown that putting Eq. (16) into Eq. (15) and carrying out the velocity-space integrals for Maxwellian f_s and $f_{s'}$, in the form of Eq. (14), yields

$$\mathbf{R}_{\mathrm{LB}}^{s-s'} = -n_s m_s \nu_{ss'} \frac{\bar{v}_T^3}{\Delta V^3} \psi\left(\frac{\Delta V^2}{\bar{v}_T^2}\right) \Delta \mathbf{V}, \tag{17}$$

in which $\Delta \mathbf{V} \equiv \mathbf{V}_s - \mathbf{V}_{s'} (\Delta V \equiv |\Delta \mathbf{V}|)$, $\bar{v}_T$ denotes an average thermal speed $\bar{v}_T \equiv \sqrt{v_{Ts}^2 + v_{Ts'}^2}$, $\nu_{ss'}$ a reference collision frequency

$$\nu_{ss'} \equiv \frac{4\pi n_{s'} q_s^2 q_{s'}^2}{m_s m_{ss'} \bar{v}_T^3} \ln \Lambda, \tag{18}$$

ψ the Maxwell integral $\psi(x) \equiv 2\int_0^x dt \sqrt{t} \exp(-t)/\sqrt{\pi}$, and $m_{ss'}$ the reduced mass $m_{ss'} \equiv m_s m_{s'}/(m_s + m_{s'})$. To connect with previous theories, like the classic work of Spitzer,[35] and to check that Eq. (17) reduces to an established result in the appropriate limit, consider the limit $\Delta V/\bar{v}_T \ll 1$. That is, a flow difference that is small compared to the average thermal speed. In this case, the small argument series expansion of ψ yields

$$\mathbf{R}_{\mathrm{LB}}^{s-s'} \approx -\frac{4}{3\sqrt{\pi}} n_s m_s \nu_{ss'} \Delta \mathbf{V}. \tag{19}$$

The Spitzer problem considers electrons slowing on ions with $T_e \approx T_i$ such that the flow is small compared to the electron thermal speed.[35] In this case $v_{Te}^2 + v_{Ti}^2 \approx v_{Te}^2$, $m_{ei} \approx m_e$, and $(V_e - V_i)/v_{Te} \ll 1$. Equation (17) predicts for this limit, $\mathbf{R}^{e-i} = -n_e m_e \nu_o (\mathbf{V}_e - \mathbf{V}_i)$, where

$$\nu_o = \frac{16\pi}{3\sqrt{\pi}} \frac{n_i Z^2 e^4 \ln \Lambda}{m_e^2 v_{Te}^3}. \tag{20}$$

This returns the Spitzer collision frequency.[35] To calculate the Spitzer resistivity, one needs to account for the affect of higher order kinetic corrections to the flow-shifted Maxwellian. Nevertheless, the simplified prediction used here is correct to within an order unity factor.

For ion-ion friction in the presheath, we are interested the limit where the difference in ion flow speeds is faster than the average thermal speed $\Delta V/\bar{v}_T \sim \mathcal{O}(T_e/T_i) \gg 1$, which is the opposite limit as the Spitzer problem. Using the asymptotic expansion for large argument in the ψ function, Eq. (17) reduces to

$$\mathbf{R}_{\mathrm{LB}}^{s-s'} \approx -n_s m_s \nu_{ss'} \frac{\bar{v}_T^3}{\Delta V^3} \Delta \mathbf{V}. \tag{21}$$

As in the Spitzer problem, this prediction of the ion-ion collisional friction would be corrected by factors of order unity due to higher order kinetic distortions of the distribution function which are not considered here.

Eq. (17) is plotted in Fig. 1 along with the asymptotic and power series expansions from Eqs. (19) and (21). For the example plasma parameters, the stable plasma contribution to the collisional friction force density is much smaller than other terms in the momentum balance equation [Eq. (11)]. For example, the $V_i dV_i/dz$ term in the momentum equation is much larger than $\mathbf{R}_{\mathrm{LB}}$: $(V_i dV_i/dz)/(n_i m_i R_{\mathrm{LB}}^{1-2}) \sim \mathcal{O}[(c_s^2/\lambda^{i-n})/(n_i m_i R_{\mathrm{LB}}^{1-2})] \sim 10$. Here we have taken the presheath length scale to be the ion-neutral collision length λ^{i-n}, which is a few centimeters in the example plasma.[3] Thus, the assumption that ion-ion collisional friction can be ignored in stable plasma seems justified.[14–18] However, it is not so small that one could claim that conventional Coulomb interactions are never important in the ion dynamics of these plasmas. It happens that it does not seem to be a significant effect for the example plasma parameters from Ref. 24. We next turn to calculating contributions to the collisional friction that arise from instability-enhanced collisions when two-stream instabilities are excited in the presheath.

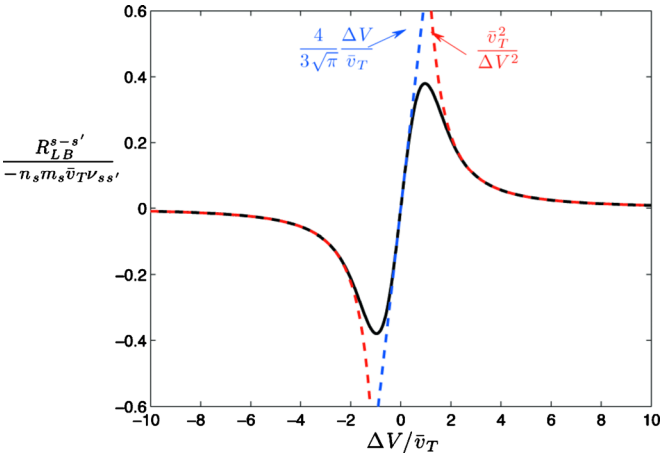

FIG. 1. (Color online) Normalized friction force density in a stable plasma between flowing Maxwellian species (solid line). The dashed lines represent the series expansion for flows slow compared to thermal speeds and the asymptotic expansion for flows fast compared to thermal speeds.

B. Instability-enhanced contribution

Calculating the instability-enhanced friction requires the plasma dielectric function, as well as the unstable mode frequency and growth rate (i.e., dispersion relation). Applying the assumption that the distribution functions of both ion species and electrons are Maxwellian, the dielectric function of Eq. (8) reduces to

$$\hat{\varepsilon}(\mathbf{k}, \omega) = 1 - \sum_s \frac{\omega_{ps}^2}{k^2 v_{Ts}^2} Z'\left(\frac{\omega - \mathbf{k} \cdot \mathbf{V}_s}{k v_{Ts}}\right), \tag{22}$$

in which Z is the plasma dispersion function[36] and the prime denotes a derivative with respect to the argument of Z.

For ion waves, it is typically assumed that $(\omega - \mathbf{k} \cdot \mathbf{V}_i)/k v_{Ti} \gg 1$ for the ion terms and $\omega/k v_{Te} \ll 1$ for electrons. This ordering is justified by the arguments that the wave phase speed is on the order of the ion sound speed and electrons are assumed to be much hotter than ions $(T_e \gg T_i)$. However, we will find that $\omega_R - \mathbf{k} \cdot \mathbf{V}_i \propto \Delta V$ for the two-stream instability, so this ordering is not valid when the difference in ion flow speeds is on the order of the ion thermal speeds: $\Delta V \sim \mathcal{O}(v_{Ti})$. Section III will discuss how to account for these finite ion temperature effects by using Eq. (22) directly. For now, we proceed to calculate the collisional friction using the conventional ordering. Using $\omega/k v_{Te} \ll 1$ and $T_i = 0$ yields the fluid plasma dielectric function

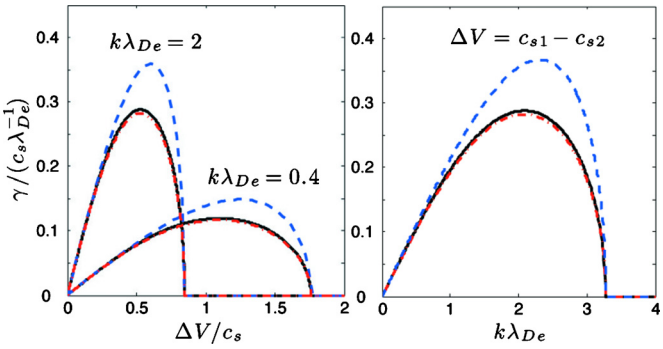

FIG. 2. (Color online) Normalized growth rates calculated for the parameters of Ref. 24 from a numerical solution of Eq. (23) (solid black line), from the quadratic approximation of Eq. (28) (dash-dotted red line) and from the approximation of Eq. (31) (dashed blue line).

$$\hat{\varepsilon}(\mathbf{k},\omega)=1-\frac{\omega_{p1}^2}{(\omega-\mathbf{k}\cdot\mathbf{V}_1)^2}-\frac{\omega_{p2}^2}{(\omega-\mathbf{k}\cdot\mathbf{V}_2)^2}+\frac{1}{k^2\lambda_{De}^2}. \quad (23)$$

Electron and ion Landau damping are both negligible in this limit. Accounting for the kinetic effect of electron Landau damping leads to an ion-acoustic instability, but this is much weaker than the two-stream fluid instabilities that we are interested in here.

Solving for the roots of Eq. (23), in order to determine the dispersion relation of the unstable modes, requires solving a quartic equation. Two of the four solutions are stable ion sound waves (with $\omega\approx kc_s$), the other two are either damped or growing ion waves [with $\omega\approx k(V_1+V_2)/2$] one of which can be unstable. The exact dispersion relation for each mode can be computed analytically from Eq. (23), but the results are so complicated that they are essentially unusable for analytically evaluating $\mathbf{R}_{\mathrm{IE}}^{s-s'}$. A numerical solution for the unstable root is shown in Fig. 2 for the example plasma parameters. In order to proceed with an analytic calculation of $\mathbf{R}_{\mathrm{IE}}^{s-s'}$, we require a simple approximation of this unstable root.

If we apply the substitution

$$\omega=\tfrac{1}{2}\mathbf{k}\cdot(\mathbf{V}_1+\mathbf{V}_2)+\mathbf{k}\cdot\Delta\mathbf{V}\Omega \quad (24)$$

to Eq. (23), the roots can be identified from the four solutions of the reduced quartic equation

$$\Omega^4-\Omega^2\left(\frac{1}{2}+a\right)-\Omega ab+\frac{1}{16}-\frac{a}{4}=0 \quad (25)$$

in which we have defined

$$a\equiv\frac{k^2c_s^2}{(\mathbf{k}\cdot\Delta\mathbf{V})^2(1+k^2\lambda_{De}^2)} \quad (26)$$

and

$$b\equiv\frac{\omega_{p1}^2-\omega_{p2}^2}{\omega_{p1}^2+\omega_{p2}^2}. \quad (27)$$

We will find for the single unstable root that $\Omega\sim b$ and $b<1$ (for the sample plasma parameters $b\approx 1/2$) so the Ω^4 term can be neglected in Eq. (25), for finding the potentially unstable root of interest. The resulting quadratic equation yields the solutions

$$\Omega=-\frac{ab\pm\sqrt{a^2b^2+(1/2+a)(1/4-a)}}{1+2a}. \quad (28)$$

Figure 2 shows that Eq. (28) provides a reasonably accurate approximation of the unstable root of Eq. (23) for the sample plasma parameters. However, Eq. (28) is still a bit complicated in its $\mathbf{k}$ dependence, and we seek a further simplified form that can be used to analytically approximate $\mathbf{R}_{\mathrm{IE}}$. Noticing that $a>1$ when $k\lambda_{De}<\sqrt{c_s^2/\Delta V^2-1}$, we can treat a as a large number for this part of k-space. Since $\Delta V\le c_{s1}-c_{s2}$ in the presheath (even in the absence of friction), this is valid for at least $k\lambda_{De}<1$ using the sample plasma parameters. In this limit, the leading term of Eq. (28) is $\Omega\approx -b/2\pm i\sqrt{\alpha}/(1+\alpha)$ which is unstable for all k in the range of validity. Here we have defined

$$\alpha\equiv\frac{n_1}{n_2}\frac{M_2}{M_1}. \quad (29)$$

When a becomes smaller than some critical value $a\le a_c$, stabilization occurs and we account for this stabilization by using the approximation $\Omega\approx -b/2\pm i\sqrt{\alpha(1-a_c/a)}/(1+\alpha)$, in which a_c is obtained from Eq. (28). This gives $1/a_c=1+\sqrt{9-8b^2}$. With these, we arrive at an approximate dispersion relation for the unstable root: $\omega=\omega_R+i\gamma$, in which

$$\omega_R\approx\mathbf{k}\cdot\left(\frac{n_2}{n_e}\frac{c_{s2}^2}{c_s^2}\mathbf{V}_1+\frac{n_1}{n_e}\frac{c_{s1}^2}{c_s^2}\mathbf{V}_2\right) \quad (30)$$

is the real part, and

$$\gamma\approx\frac{k_\parallel\Delta V\sqrt{\alpha}}{1+\alpha}\sqrt{1-\frac{k_\parallel^2\Delta V^2}{k^2\Delta V_{\mathrm{up}}^2}(1+k^2\lambda_{De}^2)} \quad (31)$$

is an expression for the growth rate. The $\parallel$ direction is along $\Delta\mathbf{V}$ and

$$\Delta V_{\mathrm{up}}^2\equiv c_s^2[1+\sqrt{1+32\alpha/(1+\alpha)^2}] \quad (32)$$

is an upper limit above which the mode stabilizes.

Fig. 2 shows that Eq. (31) can overestimate the growth rate by as much as 30%. However, it will soon be shown that this quantitative difference will not affect the conclusions drawn from the subsequent friction calculation. Applying Eq. (31) to calculate $\mathbf{R}_{\mathrm{IE}}$ leads to underestimating the minimum distance ($z_{\min}$) that waves must grow before $\mathbf{R}_{\mathrm{IE}}$ dominates by up to 30%. Correcting for this error is important only for checking that $z_{\min}$ is much shorter than the presheath scale length l. We will find that $z_{\min}/l\sim 10^{-2}$, so a 30% correction to $z_{\min}$ is irrelevant to this discussion.

In Appendix B, the instability-enhanced contribution of the collisional friction between two ion species is calculated by putting Eqs. (9), (23), (30), and (31) into Eq. (15). The result is

$$\mathbf{R}_{\mathrm{IE}}^{1-2}=-n_1m_1\nu_{12}F_{\mathrm{IE}}\Delta\mathbf{V}, \quad (33)$$

in which ν_{12} is the reference frequency from Eq. (18) and

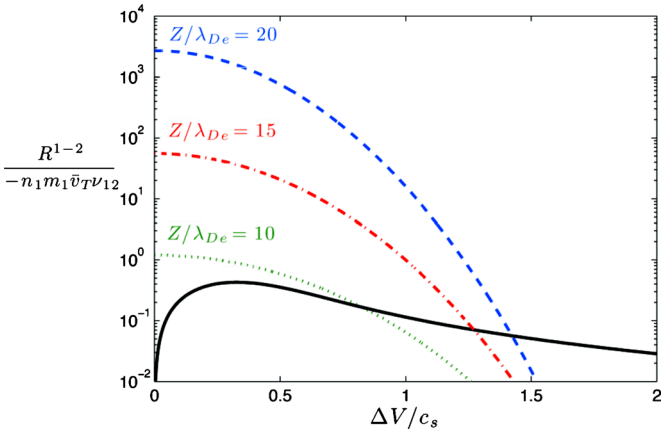

FIG. 3. (Color online) Normalized collisional friction force density for the parameters of the experiment in Ref. 24. The stable plasma contribution, calculated using Eq. (17), is shown as the black solid line. The instability-enhanced contribution from ion-ion two-stream instabilities, calculated using Eq. (33), is shown for wave growth over a distances of $Z/\lambda_{De}=10$, 15, and 20 by the dotted green line, dash-dotted red line and dashed blue line.

$$F_{\mathrm{IE}} \equiv \frac{3}{40\pi \ln\Lambda} \frac{A^{5/2} w}{4+w^{3/2}} \frac{\alpha^{5/2}}{(1+\alpha)(1-\alpha^2)^2} \frac{\bar{\nu}_T \Delta V^4}{c_s^4 \Delta V_{\mathrm{up}}} \exp\left(\frac{w}{2}\right) \tag{34}$$

is a factor that characterizes the instability-enhancement of the collisional interaction. Here, the parameters $A \equiv \Delta V_{\mathrm{up}}^2/\Delta V^2 - 1$ and

$$w \equiv \frac{2\sqrt{\alpha}}{1+\alpha} \frac{\Delta V_{\mathrm{up}}}{v_g} \left(1 - \frac{\Delta V^2}{\Delta V_{\mathrm{up}}^2}\right) \frac{Z}{\lambda_{De}}, \tag{35}$$

have been defined. The group speed for these ion-ion two-stream instabilities is

$$v_g = \frac{n_2}{n_e} \frac{c_{s,2}^2}{c_s^2} V_1 + \frac{n_1}{n_e} \frac{c_{s,1}^2}{c_s^2} V_2. \tag{36}$$

In Eq. (35), Z is a spatial variable in the $\|$ direction that takes as its origin the location that the first wave-number becomes unstable.

Unlike the calculation of Eq. (17) from Appendix A, where the only assumption made was Maxwellian distributions, the calculation of Eq. (33) in Appendix B makes use of the $T_e \gg T_i$ assumption and utilizes an integral approximation technique. One consequence of these approximations is that Eq. (33) is only valid for ion-ion instability-enhanced friction, whereas Eq. (17) can be used to calculate the stable plasma friction between any species s and s'; including ion-electron and electron-electron collisions. For this reason, we use the labels $(s=1)$ and $(s'=2)$ in Eq. (33) to specifically denote ion species.

Fig. 3 plots the instability-enhanced collisional friction from Eq. (33) for wave growth over distances of $Z/\lambda_{De}=10$, 15 and 20. For the plot, we have used $v_g \approx c_s$. Also shown is the stable plasma contribution to this friction using $\mathbf{R}_{\mathrm{LB}}^{1-2}$ from Eq. (17). Recall from Sec. II A that the stable plasma contribution to the friction force density was about an order of magnitude smaller than the other terms of the momentum balance equation for the sample plasma parameters. For instability-enhanced friction to be important requires $\mathbf{R}_{\mathrm{IE}}^{1-2}/\mathbf{R}_{\mathrm{LB}}^{1-2} \gtrsim 10$. Figure 3 shows that after growing only 20 Debye lengths, the two-stream instabilities have enhanced the collisional friction nearly 10^4 times the stable plasma level. The presheath length scale for this plasma[24] is $l \approx 5$ cm and $\lambda_{De} \approx 6\times 10^{-3}$ cm, so the wave growth distances shown in Fig. 3 are much shorter than the presheath length $Z/l \approx 10^{-2}$. Accounting for the 30% overestimation of γ from the approximation in Eq. (31) merely requires a 30% longer distance for the unstable waves to grow. Since $Z/l \approx 10^{-2}$, a 30% increase in the Z required for instability-enhanced friction to dominate is still much shorter than the presheath length. Thus, the approximations leading to Eq. (31) do not affect the central conclusion that friction from two-stream instabilities dominates within a wave growth distance that is much shorter than the presheath.

Since the $z_{\min}/l$ required for $\mathbf{R}_{\mathrm{IE}}^{1-2}$ to dominate the momentum balance equation is so small, and this frictional force is equal and opposite between the two beams [see Eq. (12)], the ΔV between ion beams cannot significantly exceed the threshold ΔV_c for which the instabilities become excited. In the cold ion limit from Eq. (31), $\Delta V_c \to 0$, so this theory predicts that each ion species should have approximately the same speed throughout the presheath, and in particular at the sheath edge. The only solution to the Bohm criterion of Eq. (2) with $V_1 = V_2$ is that each species obtain the system sound speed c_s at the sheath edge. This prediction is consistent with previous literature that reported experiments carried out in plasmas with cold ions.[19–26]

III. DETERMINING ΔV_c WITH FINITE ION TEMPERATURES

In the previous section, it was shown that if two-stream instabilities are excited in the presheath, the resultant instability-enhanced friction rapidly forces the flow speed of the two ion species together. After the instability threshold is exceeded $(\Delta V > \Delta V_c)$ the resultant force onsets sufficiently quickly and is sufficiently strong that the difference in flow speeds cannot significantly exceed the instability threshold. Thus, the condition $V_1 - V_2 = \Delta V_c$ can be used to relate the speed of the two ion species. Using this along with the generalized Bohm criterion from Eq. (2) uniquely determines the speed of each ion species at the sheath edge. Thus, an accurate prediction of the instability threshold ΔV_c is important. The previous section was based on the assumption that $T_i = 0$, in which case $\Delta V_c = 0$. In this section we go beyond the $T_i = 0$ assumption and attempt to account for finite ion temperature effects.

Finite ion temperatures can cause stabilization of the two-stream instability. Accounting for this effect allows for some separation in the ion flow speeds at the sheath edge, which alters the common sound speed solution obtained in the last section. Ion-ion two-stream instabilities have a phase speed close to the ion sound speed, so $\omega/kv_{Te} \sim \sqrt{m_e/m_i} \ll 1$ and the roots of the kinetic dielectric function from Eq. (22) solve

$$1+k^2\lambda_{De}^2=\frac{1}{2}\frac{n_1}{n_e}\frac{T_e}{T_1}Z'\left(\frac{\omega-\mathbf{k}\cdot\mathbf{V}_1}{kv_{T1}}\right)+\frac{1}{2}\frac{n_2}{n_e}\frac{T_e}{T_2}Z'\left(\frac{\omega-\mathbf{k}\cdot\mathbf{V}_2}{kv_{T2}}\right). \quad (37)$$

In the last section, it was shown that the $1+k^2\lambda_{De}^2$ term leads to stabilization at large k or large ΔV [see Eq. (31)]. Here we seek to determine a similar threshold for small ΔV (near the ion thermal speed). For determining this limit, the ion terms on the right side of Eq. (37) are larger than the $1+k^2\lambda_{De}^2$ term by $T_e/T_i \gg 1$. Thus, the left side of Eq. (37) can be neglected when determining ΔV_c. A growth rate calculation applying this approximation cannot account for the stabilization at large ΔV. Here we seek only to determine the threshold for instability at small ΔV, not a growth rate valid for large ΔV. Two approaches to this calculation are provided in this section, one is based on fluid theory and another is based on a different approximation to the kinetic plasma dispersion functions in Eq. (37). The validity of each approximation can be determined by the size of the parameter v_{T1}/v_{T2}. The fluid approach is an appropriate approximation when $v_{T1}/v_{T2} \gg 1$ or $v_{T1}/v_{T2} \ll 1$ and the kinetic approximation is appropriate when v_{T1}/v_{T2} is close to unity.

A. A fluid theory approach

A simple way to show that stabilization occurs for $\Delta V \sim \mathcal{O}(v_{Ti})$, is to use the fluid plasma dielectric function with thermal corrections.[27,37,38]

$$\hat{\varepsilon}(\mathbf{k},\omega)=1+\frac{1}{k^2\lambda_{De}^2}-\frac{\omega_{p1}^2}{(\omega-\mathbf{k}\cdot\mathbf{V}_1)^2-k^2v_{T1}^2/2}-\frac{\omega_{p2}^2}{(\omega-\mathbf{k}\cdot\mathbf{V}_2)^2-k^2v_{T2}^2/2}. \quad (38)$$

In this case, $Z'[(\omega-\mathbf{k}\cdot\mathbf{V}_i)/kv_{Ti}] \approx k^2v_{Ti}^2/[(\omega-\mathbf{k}\cdot\mathbf{V}_i)^2-k^2v_{Ti}^2/2]$ for each of the ion terms. Putting this into Eq. (37), neglecting the $1+k^2\lambda_{De}^2$ term, and applying the variable substitution from Eq. (24) yields the quadratic equation: $\bar{a}\Omega^2+\bar{b}\Omega+\bar{c}=0$. The coefficients of this quadratic are $\bar{a}\equiv\alpha+1$, $\bar{b}\equiv\alpha-1$ and

$$\bar{c}\equiv\frac{1}{4}(\alpha+1)-\frac{k^2(v_{T1}^2+\alpha v_{T2}^2)}{2k_\parallel^2\Delta V^2}. \quad (39)$$

This has an unstable solution if $\bar{b}^2-4\bar{a}\bar{c}<0$, which implies $\Delta V>(k/k_\parallel)\Delta V_c^{\mathrm{fl}}$ where

$$\Delta V_c^{\mathrm{fl}}\equiv\sqrt{\frac{1+\alpha}{2\alpha}}\sqrt{v_{T1}^2+\alpha v_{T2}^2} \quad (40)$$

is the critical difference in ion flow speeds for instability to onset.

Eq. (40) shows that the critical relative flow speed is $\mathcal{O}(v_{Ti})$. It also shows that there is a density and mass ratio [through the parameter α defined in Eq. (29)] as well as ion temperature dependence on the critical relative flow speed for instability. Equation (40) has a minimum for $\alpha=v_{T1}/v_{T2}$, which is $n_1/n_2=\sqrt{T_1/T_2}\sqrt{M_1/M_2}$. As α deviates from this value, ΔV_c^{fl} increases. If $\Delta V_c^{\mathrm{fl}}>|c_{s1}-c_{s2}|$, ion-ion streaming instabilities are not expected in the presheath. Although Eq. (40) provides a useful threshold condition for two-stream instabilities in some circumstances (when the ion masses are very different), it will be shown in the next section that the fluid approximation is not valid when the ion masses are similar. For this case, a different approximation of the kinetic formula in Eq. (37) is required.

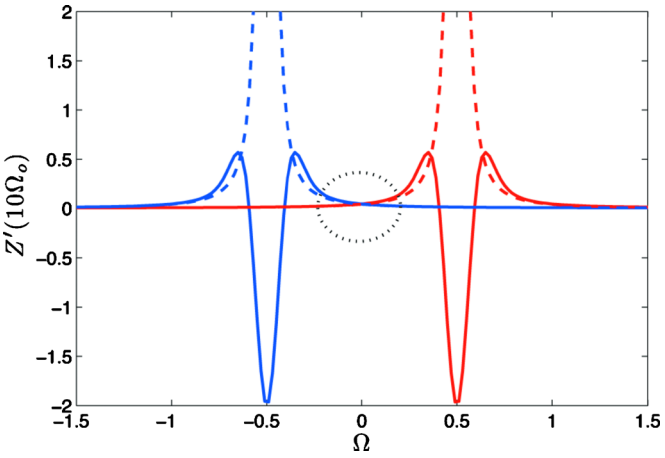

FIG. 4. (Color online) Plots of $\Re\{Z'(10\Omega_o)\}$ for $\Omega_o=\Omega-1/2$ and $\Omega_o=\Omega+1/2$ (solid lines). The 10 here is characteristic of a large ΔV since it is the coefficient representing $k_\parallel\Delta V/(kv_{Ti})$ (for each ion species). The solid lines show the real part of the exact Z' functions, and the dashed lines show the fluid approximation from Eq. (23). In this case, the fluid approximation is good near the location where the unstable roots are found. When the 10 is replaced by a number of order unity (meaning $\Delta V \sim v_{Ti}$), the two Z' functions essentially overlap, and the fluid approximation fails.

B. A kinetic theory approach

To determine whether the fluid model from Eq. (40) is valid, or a kinetic model for ΔV_c is required, consider Eq. (37). Since the left side can be neglected for $\Delta V \sim \Delta V_c \sim v_{Ti}$, we can use the following expression to calculate ΔV_c

$$\frac{n_1}{n_2}\frac{T_2}{T_1}Z'\left[\frac{\mathbf{k}\cdot\Delta\mathbf{V}(\Omega-1/2)}{kv_{T1}}\right]+Z'\left[\frac{\mathbf{k}\cdot\Delta\mathbf{V}(\Omega+1/2)}{kv_{T2}}\right]=0, \quad (41)$$

in which the substitution of Eq. (24) has also been applied. The fluid approximation used in Sec. II B is based on the large argument expansions of the Z' function. The situation appropriate to this limit is shown graphically in Fig. 4 where it is assumed that $\Delta V/v_{Ti}=10$. In this case, one of the solutions of Eq. (41) is found in the circled region where Ω is small. In this region, the real part of the Z' functions in Eq. (41) are well described by the cold fluid limit [from Eq. (23)]. Using the cold fluid model, it was shown in Eq. (31) that Ω has an imaginary component predicting growth. However, if $\Delta V/v_{Ti} \sim 1$, the fluid limit does not accurately represent the behavior of the real part of the Z' function in the region where instability is expected (for small Ω). This situation is shown in Fig. 5, in which it is assumed that $\Delta V/v_{Ti}=1$. In this regime, a different approximation technique must be used.

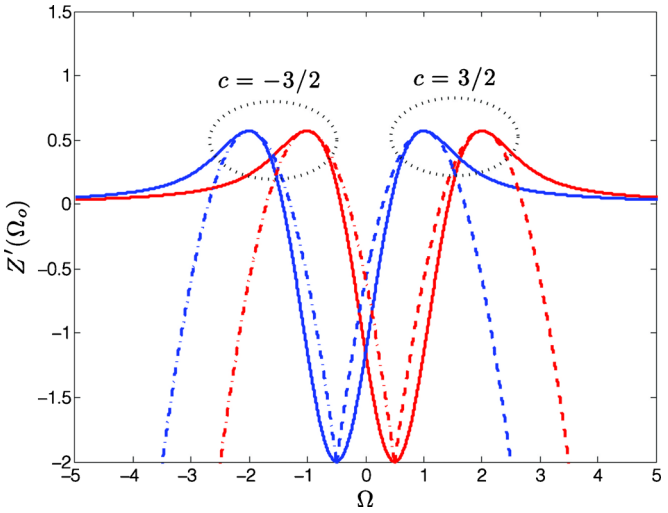

FIG. 5. (Color online) Plots of $\Re\{Z'(1\Omega_o)\}$ for $\Omega_o=\Omega-1/2$ and $\Omega_o=\Omega+1/2$ (solid lines). The 1 here is characteristic of $\Delta V\sim v_{Ti}$. The dashed lines show the expansion about the peaks for $c=\pm 3/2$.

The parameter that determines whether the fluid model from Eq. (40) is valid, or a kinetic model for ΔV_c is required is v_{T1}/v_{T2}. To show this, consider the substitution $\bar{\Omega}=(\Omega-1/2)\mathbf{k}\cdot\Delta\mathbf{V}/(kv_{T1})$. Applying this to Eq. (41) yields

$$\frac{n_1}{n_2}\frac{T_2}{T_1}Z'(\bar{\Omega})+Z'\left(\frac{v_{T1}}{v_{T2}}\bar{\Omega}+\frac{\mathbf{k}\cdot\Delta\mathbf{V}}{kv_{T2}}\right)=0. \tag{42}$$

The v_{T1}/v_{T2} term in Eq. (42) determines the width of the interior region (the region between the two maxima) of the real part of the Z' function. The $\Delta V/v_{T2}$ term determines the shift (the location of the minimum of $\Re\{Z'\}$). If $v_{T1}/v_{T2}\gg 1$, the second Z' function in Eq. (42) is very narrow and Eq. (42) can be approximated using the fluid theory (with thermal corrections) from Eq. (38). Similarly, if $v_{T1}/v_{T2}\ll 1$, the substitution $\bar{\Omega}=(\Omega+1/2)\mathbf{k}\cdot\Delta\mathbf{V}/(kv_{T2})$ shows an analogous result. Thus, Eq. (40) is a reasonable approximation if $v_{T1}/v_{T2}\gg 1$, or $v_{T1}/v_{T2}\ll 1$. From plotting a range of values, the fluid approximation qualitatively seems to be reasonable if $v_{T1}/v_{T2}\lesssim 1/4$, or $v_{T1}/v_{T2}\gtrsim 4$.

If $1/4\lesssim v_{T1}/v_{T2}\lesssim 4$, a different approximation for the Z' functions in Eq. (41) is required. For this range, consider what happens as ΔV is increased from zero. For very small ΔV, the Z' functions are very broad and the two terms of Eq. (41) essentially overlap (i.e., their maxima are very close). As ΔV increases, the real part of the two Z' functions begin to separate (i.e., the maxima become further apart), as shown in Fig. 5. Unstable roots are found when the maxima of these two functions spread far enough apart. When this occurs, one can choose more appropriate points than the small or large argument from which to expand each of the Z' functions in a Taylor series. Expanding both functions about the maxima, see Fig. 5, provides a good approximation when the ion thermal speeds are similar. We are only interested in the real part of the Z' expansion. It is expected that any instabilities driven by the imaginary contribution (i.e., inverse Landau damping) will have a much smaller growth rate than the fluid-like instabilities we are interested in here.

Expanding $Z'(w)$ in a Taylor series about an arbitrary center point $w=c$ gives

$$Z'(w)=a+b(w-c)+d(w-c)^2+\mathcal{O}\{(w-c)^3\} \tag{43}$$

where

$$a\equiv -2+2c\sqrt{\pi}e^{-c^2}\mathrm{erfi}(c)-i2c\sqrt{\pi}e^{-c^2}, \tag{44}$$

$$b\equiv 4c-(4c^2-2)\sqrt{\pi}e^{-c^2}\mathrm{erfi}(c)+i(4c^2-2)\sqrt{\pi}e^{-c^2}, \tag{45}$$

and

$$d\equiv 4(1-c^2)+(4c^3-6c)\sqrt{\pi}e^{-c^2}\mathrm{erfi}(c) -i(4c^3-6c)\sqrt{\pi}e^{-c^2}. \tag{46}$$

Here, $\mathrm{erfi}(z)=-i\mathrm{erf}(iz)$ is the "imaginary error function." For a real center point c, $\mathrm{erfi}(c)$ is also a real number.

If a center point c is specified, a, b, and d are simply numbers that can be evaluated directly from Eqs. (44)–(46). After expanding each of the Z' functions about appropriate center points, Eq. (41) reduces to a quadratic equation that can be solved analytically. For the experimental parameters that we are primarily interested in here, the ions are Ar+ and Xe+ with equal temperatures, so $v_{T1}/v_{T2}\approx\sqrt{M_2/M_1}=\sqrt{131/40}=1.8$, which is close to unity. In this case, the Z' functions have similar widths and the appropriate center points, c, are the positive peaks of each function; as shown in Fig. 5. An unstable root can arise in the region near the maxima of the Z' functions as they separate with increasing ΔV. As the maxima separate, the parabola used to model the sum of the two terms from Eq. (41) predicts an unstable root. To capture the ΔV at which this occurs, the real part of each $Z'(w)$ is expanded to quadratic order about the peaks at $w=\pm 1.502\,01\ldots$. To within 0.1% this is $\pm 3/2$. Using $c=\pm 3/2$ as the center point in Eq. (43) yields $a=0.57\mp 0.56i$, $b=0.00+1.31i$, and $d=-1.15\mp 0.84i$. The imaginary parts of a, b and d describe the kinetic effect of Landau damping (or growth). Instabilities that arise from these terms tend to be much weaker than the fluid-like instabilities that arise from the real parts. We are interested only in these faster growing instabilities here, and take only the real parts of a, b, and d. Thus, we can take

$$Z'(w)\approx a+d(w-c)^2, \tag{47}$$

in which $a=0.57$, $c=\pm 3/2$ and $d=-1.15$ to capture both of the possible locations for instability. The linear term is absent here because the real part of b is 0.00, which is expected near maxima because $\Re\{Z'\}$ is flat there.

Putting these expansions into Eq. (41), yields

$$\frac{n_1}{n_2}\frac{T_2}{T_1}\left\{a+d\left[\frac{k_\parallel \Delta V}{kv_{T1}}(\Omega-1/2)-c\right]^2\right\} + a+d\left[\frac{k_\parallel \Delta V}{kv_{T2}}(\Omega+1/2)-c\right]^2=0. \tag{48}$$

This can be written in the quadratic notation, $\bar{A}\Omega^2+\bar{B}\Omega+\bar{C}=0$, where the coefficients are

$$\bar{A}\equiv d\left[\frac{n_1}{n_2}\frac{T_2}{T_1}\frac{k_\parallel^2\Delta V^2}{k^2v_{T1}^2}+\frac{k_\parallel^2\Delta V^2}{k^2v_{T2}^2}\right], \tag{49}$$

$$\bar{B}\equiv -2d\left[\frac{n_1}{n_2}\frac{T_2}{T_1}\frac{k_\parallel \Delta V}{kv_{T1}}\left(c+\frac{1}{2}\frac{k_\parallel \Delta V}{kv_{T1}}\right)+\frac{k_\parallel \Delta V}{kv_{T2}}\left(c-\frac{1}{2}\frac{k_\parallel \Delta V}{kv_{T2}}\right)\right], \tag{50}$$

and

$$\bar{C}\equiv a\left(1+\frac{n_1}{n_2}\frac{T_2}{T_1}\right)+d\left[\frac{n_1}{n_2}\frac{T_2}{T_1}\left(c+\frac{1}{2}\frac{k_\parallel \Delta V}{kv_{T1}}\right)^2+\left(c-\frac{1}{2}\frac{k_\parallel \Delta V}{kv_{T2}}\right)^2\right]. \tag{51}$$

This quadratic has an unstable solution if $\bar{B}^2-4\bar{A}\bar{C}<0$, which implies

$$[k_\parallel \Delta V+kc(v_{T1}-v_{T2})]^2 > \frac{a}{|d|}\left(1+\frac{n_2}{n_1}\frac{T_1}{T_2}\right)\left(k^2v_{T1}^2+\frac{n_1}{n_2}\frac{T_2}{T_1}k^2v_{T2}^2\right). \tag{52}$$

Here we have used the fact that $d<0$ to write $d=-|d|$.

Eq. (52) predicts instability if $\Delta V>(k/k_\parallel)\Delta V_c^{\rm kin}$, in which

$$\Delta V_c^{\rm kin}\approx -\frac{3}{2}|v_{T2}-v_{T1}| + \sqrt{\frac{1}{2}\left(1+\frac{n_2}{n_1}\frac{T_1}{T_2}\right)\left(v_{T1}^2+\frac{n_1}{n_2}\frac{T_2}{T_1}v_{T2}^2\right)}. \tag{53}$$

Here we have applied the $c=\pm 3/2$ center point, for which $a/|d|=0.57/1.15\approx 1/2$ (to within 0.4%).

IV. HOW FRICTION CAN DETERMINE THE BOHM CRITERION

It was shown in Sec. II B that when ion-ion two-stream instabilities onset, the friction between ion species rapidly (within several Debye lengths) forces the species together. This instability-enhanced friction causes the momentum balance equation to be stiff, whereby the difference in ion flow speeds essentially cannot exceed the marginal value for instability onset (ΔV_c). If instabilities are present, this critical speed provides an equation relating the flow speed of each species: $V_1-V_2=\Delta V_c$. If $\Delta V_c>|c_{s1}-c_{s2}|$, two-stream instabilities are not expected to be excited in the presheath and the collisionless solution with $V_1-V_2=c_{s1}-c_{s2}$ is expected to hold (in the absence of significant ion-neutral friction forces[14–18]). Putting these together, the condition $V_1-V_2=\Delta V_c$

$$\Delta V_c\equiv\begin{cases}\Delta V_c^{\rm fl}, \text{ or } \Delta V_c^{\rm kin} & \text{if} \le |c_{s1}-c_{s2}|\\ c_{s1}-c_{s2} & \text{if} > |c_{s1}-c_{s2}|\end{cases} \tag{54}$$

provides an expression relating V_1 and V_2 at the sheath edge. Here $\Delta V_c^{\rm fl}$ is the fluid estimate for the instability threshold from Eq. (40), which is expected to be valid if v_{T1}/v_{T2} is very large or small, and $\Delta V_c^{\rm kin}$ is a kinetic estimate from Eq. (53) for the $v_{T1}/v_{T2}\approx 1$ regime. The Bohm criterion of Eq. (2) provides a second equation that closes this system. Thus, with two equations we can solve for the two unknowns V_1 and V_2. In this way, instability-enhanced friction can provide a unique determination of the solutions to the two-species Bohm criterion.

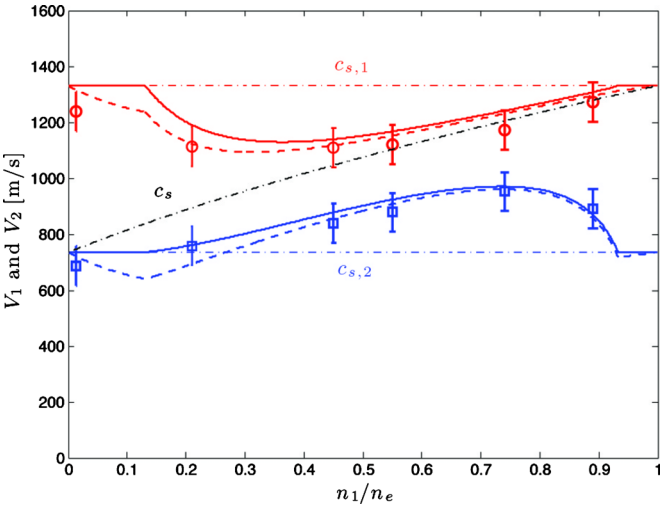

FIG. 6. (Color online) Plot of the predicted and measured ion flow speeds at the sheath edge of an Ar+ (labeled 1 and shown in red) and Xe+ (labeled 2 and shown in blue) plasma. The solid lines show the theoretical prediction using Eq. (53) in Eq. (54), and numerically solving the quartic Eq. (55). The dashed lines show the predictions of a simplified model that uses a linear approximation of the quartic [Eqs. (58) and (59)]. The data points are from experimental measurements of Yip, Hershkowitz, and Severn from Ref. 29. Also shown are the individual sound speeds (dash-dotted red and blue lines) and the system sound speed (dash-dotted black line).

Putting Eq. (58) into the Bohm criterion of Eq. (2) yields

$$\frac{n_1}{n_e}\frac{c_{s1}^2}{V_1^2}+\frac{n_2}{n_e}\frac{c_{s2}^2}{(V_1-\Delta V_c)^2}=1, \tag{55}$$

which is a quartic equation to solve for V_1. Two of the solutions are imaginary, one is real and negative, and one is real and positive. Only the real positive solution is physically relevant. A full solution of this equation requires solving the quartic, which can be done analytically, but the result is a complicated equation. A numerical solution to Eq. (55) for the sample plasma parameters is shown as a function of n_1/n_e in Fig. 6. The general solution has the property that the speed of each ion species approaches its individual sound speed for $n_1/n_2\ll 1$, and $n_1/n_2\gg 1$, and that the speeds are closer to the system sound speed for $n_1/n_2\approx 1$.

A simple linear approximation of the quartic can be developed as follows. From Eq. (40) or Eq. (53), it is expected

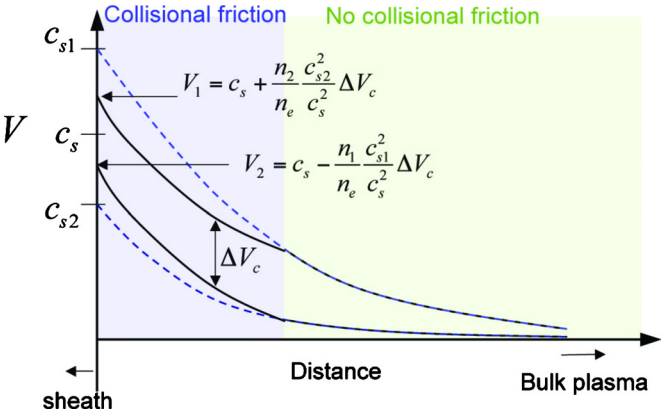

FIG. 7. (Color online) Sketch of predicted ion fluid speed profiles through the presheath. There is a region with negligible ion-ion collisional friction near the bulk plasma, and a region where instability-enhanced friction is important near the sheath.

that $\Delta V_c \sim \mathcal{O}(v_{Ti}) \ll V_1$, $V_2 \sim c_s$, so Eq. (55) can be expanded in a series for $\Delta V_c \ll V_1$. Keeping the lowest order ΔV_c correction yields

$$\frac{c_s^2}{V_1^2} + 2\frac{n_2}{n_e}c_{s2}^2\frac{\Delta V_c}{V_1^3} \approx 1, \tag{56}$$

in which the system sound speed $c_s \equiv \sqrt{n_1 c_{s1}^2 + n_2 c_{s2}^2}/\sqrt{n_e}$, has been identified using Eq. (5).

Next, we apply the substitution $V_1 = c_s + v_\epsilon$ and seek v_ϵ. Putting this into Eq. (56) yields

$$2c_s^2 v_\epsilon + 3c_s v_\epsilon^2 + v_\epsilon^3 = 2\frac{n_2}{n_e}c_{s2}^2\Delta V_c. \tag{57}$$

Equation (57) shows that $v_\epsilon \sim \Delta V_c \sim \mathcal{O}(v_{Ti})$, which is small compared to c_s. Neglecting the v_ϵ^2 and v_ϵ^3 terms compared to the v_ϵ terms yields $v_\epsilon = n_2 c_{s2}^2/(n_e c_s^2)\Delta V_c$. Thus, we have

$$V_1 \approx c_s + \frac{n_2}{n_e}\frac{c_{s2}^2}{c_s^2}\Delta V_c. \tag{58}$$

Putting this into $V_1 - V_2 = \Delta V_c$ yields

$$V_2 \approx c_s - \frac{n_1}{n_e}\frac{c_{s1}^2}{c_s^2}\Delta V_c. \tag{59}$$

Equations (58) and (59) show that accounting for finite (but still small) ion temperatures leads to the result that the flow speed of each ion species at the sheath edge is close to the system sound speed c_s. Differences from the common sound speed are determined by the thermal speed and the density of each ion species. A schematic depiction of the presheath for this situation is shown in Fig. 7. Here ions enter the presheath with a small and similar flow speed. As the presheath electric field accelerates them, the lighter species obtains a larger flow speed than the heavier species. When the difference in flow speeds exceeds ΔV_c, instability-enhanced friction rapidly forces the two species back toward the threshold $\Delta V = \Delta V_c$. From this point to the sheath edge, the difference in ion flow speeds is "locked" to $\Delta V = \Delta V_c$. This "locking" feature can be seen in previous LIF measurements of ion fluid speeds in a presheath.[24]

The density dependence of ΔV_c provides a convenient parameter that can be varied in experiments to test the theory. Such an experiment has already been performed by Yip, Hershkowitz, and Severn[29] (using LIF) in an $Ar^+ - Xe^+$ plasma. A comparison of their measurements to the theoretical predictions presented here is shown in Fig. 6. The relevant temperatures from the experiment were $T_1 \approx T_2 = 0.04$ eV and $T_e = 0.7$ eV (in the theory curves we do not account for the slight change in ion temperatures that was measured in the experiment as n_1/n_e varied). In Fig. 6, Ar+ ions are labeled as species 1 and Xe+ ions as species 2. Since $v_{T1}/v_{T2} \approx 1.8 \sim 1$, Eq. (53) is the appropriate expression to use for ΔV_c for this experiment. Figure 6 shows the theoretical prediction using Eq. (53) in Eq. (54), and numerically solving the quartic Eq. (55). It also shows the theoretical prediction using the linear approximation of the quartic from Eqs. (58) and (59). As ΔV_c increases and approaches $c_{s1} - c_{s2}$, the linear approximation can give an unphysical prediction that the Xe+ ions are slower than their own sound speed. However, the full quartic solution shows that this is a byproduct of the linear approximation and not a feature of the theory. The linear approximation agrees well with the full numerical solution for smaller ΔV_c.

Fig. 6 shows that the experimental data agree with the theory over the whole range of ion density ratios. It also shows that the previous theoretical predictions that each ion species obtains its individual sound speed,[14–18] or that each ion species obtains the common system sound speed[27] do not agree with the experiments over this whole range. The individual sound speed solution does work when n_1/n_2 is either large or small. In this situation, two-stream instabilities are not expected, so $\Delta V \approx c_{s1} - c_{s2}$. Conversely, the individual ion speeds approach the system sound speed when the ion density ratio is near 1 (in the plot, $n_1/n_e = 1/2$). In this case, theory predicts that instability-enhanced friction will be present for a small, but finite, difference in ion flow speeds. Thus, the results of previous theories can be recovered in different density ratio limits. The prediction that the ion flow speed at the sheath edge depends on the density ratio is a new theoretical result. Other recent experiments[39] have been conducted at sufficiently high ion temperatures that two-stream instabilities are not expected to be excited in the presheath. These found that the ions approach their individual sound speeds at the sheath edge, which is consistent with the theory presented here.

V. SUMMARY

The Bohm criterion [Eq. (2)] provides a single constraint on the possible flow speeds of ions at the sheath edge. If the plasma contains two (or more) ion species, this single constraint does not uniquely determine the flow speed of each ion species. The majority of previous theoretical work predicts that each ion species should approach its individual sound speed ($c_{s,i}$) at the sheath edge.[14–18] This work neglected collisional coupling between the ion species. However, recent experiments in $Ar^+ - Xe^+$ plasmas have measured the ion flow speeds to be much closer to a common speed,

which is the system sound speed c_s, at the sheath edge. These measurements suggest that a frictional force may be acting between the ion species.

It was shown in Sec. II A that the ion-ion frictional force in a stable plasma is too weak to explain the experimental results. However, Sec. II B showed that ion-ion two-stream instabilities can significantly enhance the frictional force between ion species. Ion-ion two-stream instabilities can be excited in the presheath if the electrons are much hotter than the ions and the difference in fluid flow speeds between the ion species exceeds a critical value: $V_1-V_2=\Delta V\geq\Delta V_c$. When this threshold is surpassed, the frictional force between ion species is enhanced by upwards of four orders of magnitude within a distance of tens of Debye lengths. Since this enhanced frictional force becomes so strong within such a short distance (compared to the presheath length, which is thousands of Debye lengths), it creates a very stiff system whereby if the instability onset condition ($\Delta V\geq\Delta V_c$) is exceeded, the resultant force rapidly pushes the flow speeds back to the marginal condition for instability onset. Thus, in plasmas with ion-ion two-stream instabilities in the presheath, instability-enhanced friction provides the restriction $V_1-V_2=\Delta V_c$. Using this condition in conjunction with the Bohm criterion for two ion species plasmas uniquely determines the flow speed of each ion species at the sheath edge. The challenge then is to determine ΔV_c for given plasma parameters.

The instability onset condition (ΔV_c) is determined from the wave dispersion relation [roots of the plasma dielectric function $\hat{\varepsilon}(\mathbf{k},\omega)=0$] by finding the location where the growth rate (γ) becomes positive. Using a fluid model of the plasma that assumes ions are cold, it was shown in Sec. II B that $\Delta V_c\to 0$. Using the condition $\Delta V=0$ in the Bohm criterion leads to the prediction that the flow speed of each ion species reaches a common system sound speed at the sheath edge $V_1=V_2=c_s$. However, in many plasmas finite ion temperature effects can significantly change ΔV_c.

In Sec. III, approximate formula for ΔV_c were derived that account for finite ion temperature effects. A fluid model of the plasma dielectric function was used to show that $\Delta V_c\sim\mathcal{O}(v_{Ti})$ and that ΔV_c depends on the ratio of densities of the two ion species as well as their thermal speeds. This result, Eq. (40), has the trend that ΔV_c has a minimum for $n_1/n_2\sim 1$, and gets larger as n_1/n_2 deviates from unity. If $\Delta V_c>|c_{s,1}-c_{s,2}|$, no two-stream instabilities will be excited. In this case, collisional coupling between ion species is negligible and the conventional solution that each ion species reaches its individual sound speed at the sheath edge is expected to hold.

Although the fluid model of the plasma dielectric predicts many important features of ΔV_c, it is only expected to hold when $v_{T1}/v_{T2}\gg 1$, or $v_{T1}/v_{T2}\ll 1$. A different approximation of the kinetic dielectric function is required for $v_{T1}/v_{T2}\sim 1$. Section III provided an estimate for this regime based on a series expansion of the plasma dispersion function. This estimate made a number of assumptions. The ion distribution functions were assumed to be Maxwellian to arrive at the plasma dispersion function representation. Furthermore, the series approximation scheme is limited by the restriction $v_{T1}/v_{T2}\approx 1$. Accurately accounting for intermediate values of v_{T1}/v_{T2}, or for deviations from Maxwellians, requires a different theoretical evaluation of the full dielectric function from Eq. (8) for the particular plasma parameters of interest.

The difference in flow speeds at the sheath edge is given by the minimum of ΔV_c or $|c_{s,1}-c_{s,2}|$. Using this expression for ΔV in the two-species Bohm criterion yields a quartic equation for V_1 or V_2. Only one of the four solutions of this equation gives a physically meaningful real, positive result for the flow speeds. Section IV shows that if ΔV_c is much smaller than $|c_{s,1}-c_{s,2}|$ that this quartic equation can be well approximated by just the linear term. This leads to the results of Eqs. (58) and (59), where the speed of each ion species is the common system sound speed plus a correction term that depends on the density of the ion species and ΔV_c. This result provides a handy formula, but a more accurate solution for $\Delta V_c\sim\mathcal{O}(|c_{s,1}-c_{s,2}|)$ requires solving the whole quartic equation. In Fig. 6, the predictions of this theory are shown to compare well to recent LIF experiments[29] of the ion flow speeds in an Ar^+–Xe^+ plasma. The prediction that the ion flow speeds depend on the ion concentration is a new theoretical result.

ACKNOWLEDGMENTS

The authors thank J. D. Callen for helpful discussions on this work and C.-S. Yip, N. Hershkowitz, and G. D. Severn for providing data from Ref. 29, which was used in Fig. 6. This material is based upon work supported under a National Science Foundation Graduate Research Fellowship (SDB.) and by the U.S. Department of Energy under Grant No. DE-FG02-86ER53218.

APPENDIX A: CALCULATION OF $\mathbf{R}_{\mathrm{LB}}^{s-s'}$

Here we calculate $\mathbf{R}_{\mathrm{LB}}^{s-s'}$ by putting Eq. (16) into (15) assuming f_s and $f_{s'}$ are both flow-shifted Maxwellians: $f_s=n_s\exp[-(\mathbf{v}-\mathbf{V}_s)^2/v_{Ts}^2]/(\pi^{3/2}v_{Ts}^3)$. Using the fact that $\mathcal{Q}_{\mathrm{LB}}^{s-s'}\cdot\mathbf{u}=0$, and that $\mathcal{Q}_{\mathrm{LB}}^{s-s'}$ is a function of $\mathbf{u}$ only, Eq. (15) can be written

$$\mathbf{R}_{\mathrm{LB}}^{s-s'}=-m_s\int d^3u\,\mathcal{Q}_{\mathrm{LB}}^{s-s'}\cdot\left[\left(\frac{1}{T_{s'}}-\frac{1}{T_s}\right)\mathbf{I}_1+\left(\frac{\mathbf{V}_s}{T_s}-\frac{\mathbf{V}_{s'}}{T_{s'}}\right)I_2\right],\tag{A1}$$

in which we have defined the integrals

$$\mathbf{I}_1\equiv\int d^3v'\mathbf{v}'f_{s'}(\mathbf{v}')f_s(\mathbf{u}+\mathbf{v}')=\frac{n_sn_{s'}}{\pi^{3/2}\bar{v}_T^5}\left\{(v_{Ts'}^2\mathbf{V}_s+v_{Ts}^2\mathbf{V}_{s'})\times\exp\left[-\frac{(\mathbf{u}-\Delta\mathbf{V})^2}{\bar{v}_T^2}\right]-v_{Ts'}^2\mathbf{u}\right\}\tag{A2}$$

and

$$I_2 \equiv \int d^3v' f_{s'}(\mathbf{v}') f_s(\mathbf{u}+\mathbf{v}') = \frac{n_s n_{s'}}{\pi^{3/2}\bar{v}_T^3}\exp\left[-\frac{(\mathbf{u}-\Delta\mathbf{V})^2}{\bar{v}_T^2}\right]. \tag{A3}$$

Here $\bar{v}_T \equiv \sqrt{v_{Ts}^2+v_{Ts'}^2}$ is an average thermal speed and $\Delta\mathbf{V}\equiv\mathbf{V}_s-\mathbf{V}_{s'}$. Putting Eqs. (A2) and (A3) into Eq. (A1), and again applying $\mathcal{Q}_{\mathrm{LB}}^{s-s'}\cdot\mathbf{u}=0$, yields

$$\mathbf{R}_{\mathrm{LB}}^{s-s'} = -\frac{2n_s n_{s'} m_s}{\pi^{3/2} m_{ss'}\bar{v}_T^5} \times \int d^3u \mathcal{Q}_{\mathrm{LB}}^{s-s'}\cdot\Delta\mathbf{V}\exp\left[-\frac{(\mathbf{u}-\Delta\mathbf{V})^2}{\bar{v}_T^2}\right], \tag{A4}$$

in which $m_{ss'}\equiv m_s m_{s'}/(m_s+m_{s'})$ is the reduced mass.

We apply a cylindrical coordinate system for $\mathbf{u}$, with the notation $\mathbf{u}=u_x\hat{x}+u_y\hat{y}+u_z\hat{z}$ where $u_x=u_\perp\cos\psi$, $u_y=u_\perp\sin\psi$, and $u_z=u_\parallel$ and choose the parallel direction to be aligned with $\Delta\mathbf{V}$. Putting Eq. (16) into Eq. (A4), we find that the components of $\mathbf{R}_{\mathrm{LB}}^{s-s'}$ perpendicular to $\Delta\mathbf{V}$ vanish due to odd parity of the u_x or u_y integrals. This is expected physically because there is no flow in these perpendicular directions to cause any frictional force. We are then left with

$$\mathbf{R}_{\mathrm{LB}}^{s-s'} = -\frac{4n_s n_{s'} q_s^2 q_{s'}^2 \ln\Lambda}{\sqrt{\pi} m_{ss'}\bar{v}_T^5}\Delta\mathbf{V} I_3, \tag{A5}$$

in which the integral

$$I_3 \equiv \int d^3u \frac{u_\perp^2}{u^3}\exp\left[-\frac{u_\perp^2+(u_\parallel-\Delta V)^2}{\bar{v}_T^2}\right] \tag{A6}$$

has been defined.

The azimuthal part of the u integral in Eq. (A6) simply gives a 2π. After evaluating the $u_\perp$ component, we are left with $I_3=2\pi(-I_4+I_5)$, where

$$I_4 \equiv \int_{-\infty}^{\infty} du_\parallel |u_\parallel| \exp\left[-\frac{(u_\parallel-\Delta V)^2}{\bar{v}_T^2}\right]. \tag{A7}$$

and

$$I_5 = \frac{\sqrt{\pi}}{2}\bar{v}_T e^{-\Delta V^2/\bar{v}_T^2}\int_{-\infty}^{\infty} du_\parallel\left(1+2\frac{u_\parallel^2}{\bar{v}_T^2}\right) \times \exp\left(\frac{2\Delta V u_\parallel}{\bar{v}_T^2}\right)\mathrm{erfc}\left(\frac{|u_\parallel|}{\bar{v}_T}\right).$$

I_4 can be evaluated by splitting the limits of integration for the positive and negative intervals and using integration by parts to give $I_4=\sqrt{\pi}\bar{v}_T\Delta V\,\mathrm{erf}(\Delta V/\bar{v}_T)+\bar{v}_T^2\exp(-\Delta V^2/\bar{v}_T^2)$. I_5 can be written in terms of cosh

$$I_5 = \sqrt{\pi}\bar{v}_T^2\exp\left(-\frac{\Delta V^2}{\bar{v}_T^2}\right) \times \int_0^\infty dy(1+2y^2)\cosh\left(2\frac{\Delta V}{\bar{v}_T}y\right)\mathrm{erfc}(y). \tag{A8}$$

Equation (A8) can then be evaluated using integration-by-parts, which yields

$$I_5 = \bar{v}_T^2\left(1-\frac{\bar{v}_T^2}{\Delta V^2}\right)e^{-\Delta V^2/\bar{v}_T^2}+\sqrt{\pi}\bar{v}_T^2\,\mathrm{erf}\left(\frac{\Delta V}{\bar{v}_T}\right) \times\left(\frac{\Delta V}{\bar{v}_T}+\frac{1}{2}\frac{\bar{v}_T^3}{\Delta V^3}\right). \tag{A9}$$

Thus, we find

$$I_3 = \pi^{3/2}\frac{\bar{v}_T^5}{\Delta V^3}\psi\left(\frac{\Delta V^2}{\bar{v}_T^2}\right), \tag{A10}$$

in which ψ is the Maxwell integral. Finally, putting Eq. (A10) into Eq. (A5) gives

$$\mathbf{R}_{\mathrm{LB}}^{s-s'} = -\frac{4\pi q_s^2 q_{s'}^2 n_s n_{s'}\ln\Lambda}{m_{ss'}\bar{v}_T^3}\frac{\bar{v}_T^3}{\Delta V^3}\psi\left(\frac{\Delta V^2}{\bar{v}_T^2}\right)\Delta\mathbf{V}, \tag{A11}$$

which completes this derivation of Eq. (17).

APPENDIX B: CALCULATION OF $\mathbf{R}_{\mathrm{IE}}^{1-2}$

Here we calculate $\mathbf{R}_{\mathrm{IE}}^{1-2}$ by putting Eqs. (9), (23), (30), and (31) into Eq. (15). We assume that the ion distributions f_1 and f_2 are both flow-shifted Maxwellians with temperatures much colder than the electron temperature. Unlike $\mathcal{Q}_{\mathrm{LB}}^{s-s'}$, $\mathcal{Q}_{\mathrm{IE}}^{s-s'}$ is not proportional to $\delta(\mathbf{k}\cdot\mathbf{u})$. However, it has been shown that if $\gamma/\omega_R\ll 1$, it can be written in such a form.[34] Since this condition is met for the two-stream instabilities of interest here, we utilize the property $\mathcal{Q}_{\mathrm{IE}}^{1-2}\cdot\mathbf{u}\approx 0$, to write Eq. (15) as

$$\mathbf{R}_{\mathrm{IE}}^{1-2} = -m_1\int d^3u\int d^3v' f_1(\mathbf{u}+\mathbf{v}')f_2\mathbf{v}'\mathcal{Q}_{\mathrm{IE}}^{1-2} \cdot\left[\left(\frac{1}{T_2}-\frac{1}{T_1}\right)\mathbf{v}'+\left(\frac{\mathbf{V}_1}{T_1}-\frac{\mathbf{V}_2}{T_2}\right)\right]. \tag{B1}$$

It is very difficult to evaluate the velocity-space integrals in Eq. (B1) directly. We seek to approximate these integrals. Since v_{T1}, $v_{T2}\ll c_{s,1}$, $c_{s,2}\sim V_1$, V_2, the ion distribution functions are very localized in velocity space about the flow speeds V_1 and V_2. We use this to apply the approximation $\mathcal{Q}_{\mathrm{IE}}^{1-2}(\mathbf{v},\mathbf{v}')\approx\mathcal{Q}_{\mathrm{IE}}^{1-2}(\mathbf{V}_1,\mathbf{V}_2)$. Thus, the instability-enhanced collisional kernel from Eq. (9) is approximately

$$\mathcal{Q}_{\mathrm{IE}}^{1-2} \approx \frac{2q_1^2q_2^2}{\pi m_1}\int d^3k\frac{\mathbf{kk}}{k^4} \times\frac{\gamma\exp(2\gamma t)/|\partial\hat{\varepsilon}/\partial\omega|_{\omega_R}^2}{[(\omega_R-\mathbf{k}\cdot\mathbf{V}_1)^2+\gamma^2][(\omega_R-\mathbf{k}\cdot\mathbf{V}_2)^2+\gamma^2]}. \tag{B2}$$

Using Eqs. (A2) and (A3), the remaining velocity-space integrals of Eq. (B1) can be evaluated directly

$$\int d^3u d^3v' \left[\left(\frac{1}{T_2} - \frac{1}{T_1} \right) \mathbf{v}' + \left(\frac{\mathbf{V}_1}{T_1} - \frac{\mathbf{V}_2}{T_2} \right) \right] f_2(\mathbf{v}') f_1(\mathbf{u}+\mathbf{v}') = \frac{2n_1 n_2}{m_{12}\bar{v}_T^2} \Delta \mathbf{V} \tag{B3}$$

in which $\bar{v}_T$ is the average ion thermal speed and m_{12} is the reduced mass. Putting Eqs. (B2) and (B3) into Eq. (B1), and applying the assumption $\omega_R - \mathbf{k}\cdot\mathbf{V} \ll \gamma$, yields

$$\mathbf{R}_{\mathrm{IE}}^{1-2} \approx -\frac{4q_1^2 q_2^2 n_1 n_2}{\pi m_{12}\bar{v}_T^2} \int d^3k \frac{\mathbf{k}\mathbf{k}\cdot\Delta\mathbf{V}}{k^4} \times \frac{\gamma \exp(2\gamma t)/\left|\partial\hat{\varepsilon}/\partial\omega\right|_{\omega_R}^2}{(\omega_R - \mathbf{k}\cdot\mathbf{V}_1)^2(\omega_R - \mathbf{k}\cdot\mathbf{V}_2)^2}. \tag{B4}$$

Next, we insert the plasma dielectric properties from Eqs. (23), (30), and (31) into Eq. (B4). Taking the derivative of $\hat{\varepsilon}$ from Eq. (23) with respect to ω yields

$$\frac{\partial\hat{\varepsilon}}{\partial\omega} = \frac{2\omega_{p1}^2}{(\omega - \mathbf{k}\cdot\mathbf{V}_1)^3} + \frac{2\omega_{p2}^2}{(\omega - \mathbf{k}\cdot\mathbf{V}_2)^3}. \tag{B5}$$

The real part of the unstable wave frequency, from Eq. (30), can be written in the alternative form

$$\omega_R = \tfrac{1}{2}k_\parallel[V_1(1+\beta) + V_2(1-\beta)] \tag{B6}$$

in which we have defined

$$\beta \equiv \frac{n_2}{n_e}\frac{c_{s2}^2}{c_s^2} - \frac{n_1}{n_e}\frac{c_{s1}^2}{c_s^2}. \tag{B7}$$

The $\parallel$ direction is aligned with $\Delta\mathbf{V}$. With this identification:

$$\omega_R - \mathbf{k}\cdot\mathbf{V}_1 = -\tfrac{1}{2}(1-\beta)\mathbf{k}\cdot\Delta\mathbf{V} \tag{B8}$$

and

$$\omega_R - \mathbf{k}\cdot\mathbf{V}_2 = \tfrac{1}{2}(1+\beta)\mathbf{k}\cdot\Delta\mathbf{V}. \tag{B9}$$

Putting these into Eq. (B5), and squaring the result, yields

$$\left|\frac{\partial\hat{\varepsilon}}{\partial\omega}\right|_{\omega_R}^2 = \frac{256}{(\mathbf{k}\cdot\Delta\mathbf{V})^6}\left[\frac{\omega_{p1}^2}{(\beta-1)^3} + \frac{\omega_{p2}^2}{(\beta+1)^3}\right]^2. \tag{B10}$$

For convective instabilities, such as the two-stream instability we are concerned with here, time in the $2\gamma t$ term must be calculated in the rest frame of the wave. Since these waves propagate as they grow, their amplitude changes at each spatial location, rather than in time at a fixed spatial location. Formally, this time can be written[33]

$$2\gamma t = 2\int_{\mathbf{x}_o(\mathbf{k})}^{\mathbf{x}} d\mathbf{x}' \cdot \frac{\mathbf{v}_g \gamma}{|\mathbf{v}_g|^2}, \tag{B11}$$

in which

$$\mathbf{v}_g = \frac{\partial\omega_R}{\partial\mathbf{k}} = \frac{1}{2}[\mathbf{V}_1(1+\beta) + \mathbf{V}_2(1-\beta)] \tag{B12}$$

is the group velocity, $\mathbf{x}_o(\mathbf{k})$ is the location in space where wavevector $\mathbf{k}$ becomes unstable, and the integral $d\mathbf{x}'$ is taken along the path of the mode. In principle, the spatial integral in Eq. (B11) requires integrating the profile of γ and $\mathbf{v}_g$, which change through the presheath due to variations in the ion fluid speeds and densities. It also requires knowing the spatial location $\mathbf{x}_o(\mathbf{k})$ at which each wavevector $\mathbf{k}$ becomes excited. In estimating Eq. (B11), we assume that changes from spatial variations are weak, and we account for $\mathbf{x}_o(\mathbf{k})$ by only integrating over the unstable $\mathbf{k}$ for each spatial location $\mathbf{x}$. Following these approximations we obtain

$$2\gamma t \approx \frac{2Z\gamma}{v_g}, \tag{B13}$$

in which Z is a shifted coordinate (with respect to z) that takes as its origin the location where the first instability onset occurs. In this case, $Z=0$ will be the presheath-plasma boundary.

The growth rate from Eq. (31) can be written

$$\gamma = \frac{k_\parallel \Delta V^2}{\Delta V_{\mathrm{up}}}\frac{\sqrt{\alpha}}{1+\alpha}\sqrt{A - k_\parallel^2\lambda_{De}^2}, \tag{B14}$$

in which $A \equiv \Delta V_{\mathrm{up}}^2/\Delta V^2 - 1$. Putting Eq. (B14) into Eq. (B13) yields

$$2\gamma t \approx \frac{2\gamma Z}{v_g} = W k_\parallel \lambda_{De}\sqrt{A - k_\parallel^2\lambda_{De}^2}, \tag{B15}$$

in which

$$W \equiv \frac{2\sqrt{\alpha}}{1+\alpha}\frac{\Delta V^2}{v_g \Delta V_{\mathrm{up}}}\frac{Z}{\lambda_{De}}. \tag{B16}$$

Using cylindrical polar coordinates $\mathbf{k} = k_\perp \cos\theta\hat{x} + k_\perp \sin\theta\hat{y} + k_\parallel\hat{z}$, the $\mathbf{k}\mathbf{k}\cdot\Delta\mathbf{V}$ term in Eq. (B4) can be written $\mathbf{k}\mathbf{k}\cdot\Delta\mathbf{V} = (k_\parallel k_\perp \cos\theta\hat{x} + k_\parallel k_\perp \sin\theta\hat{y} + k_\parallel^2\hat{z})\Delta V$. Noticing that this is the only place that the azimuthal dependence of $\mathbf{k}$ shows up in the k-space integral of Eq. (B4) (since γ, ω_R and $|\partial\hat{\varepsilon}/\partial\omega|_{\omega_R}^2$ are only functions of $|\mathbf{k}|$ and $k_\parallel$), the terms in the $\hat{x}$ and $\hat{y}$ directions (proportional to $\cos\theta$ and $\sin\theta$) will vanish upon integrating over θ. This is expected from physical grounds since there is no flow in these directions to drive a frictional force. Putting Eqs. (B8)–(B10), (B14), and (B15), into Eq. (B4), and evaluating the trivial θ integral, yields

$$\mathbf{R}_{IE}^{1-2} = -\frac{q_1^2 q_2^2 n_1 n_2}{2m_{12}\bar{v}_T^2}\frac{\sqrt{\alpha}}{1+\alpha} \times \frac{(1-\beta^2)^4}{[\omega_{p1}^2(\beta+1)^3 + \omega_{p2}^2(\beta-1)^3]^2}\frac{\Delta V^4 \Delta\mathbf{V}}{\Delta V_{\mathrm{up}}} I, \tag{B17}$$

in which

$$I \equiv \int_{-k_c}^{k_c} dk_\parallel k_\parallel^5 \sqrt{A - k_\parallel^2\lambda_{De}^2} \times \exp(W k_\parallel \lambda_{De}\sqrt{A - k_\parallel^2\lambda_{De}^2}) \int_0^\infty dk_\perp \frac{k_\perp}{k^4}. \tag{B18}$$

The bound on $k_\parallel$ has been imposed to restrict the integration domain to unstable $k_\parallel$: $k_c = \sqrt{A}/\lambda_{De}$. Part of the approximation of $2\gamma t$ from Eq. (B13) was to integrate only the unstable region of k-space.

Next, we estimate the integral I from Eq. (B18). The $k_\perp$ integral can be integrated analytically

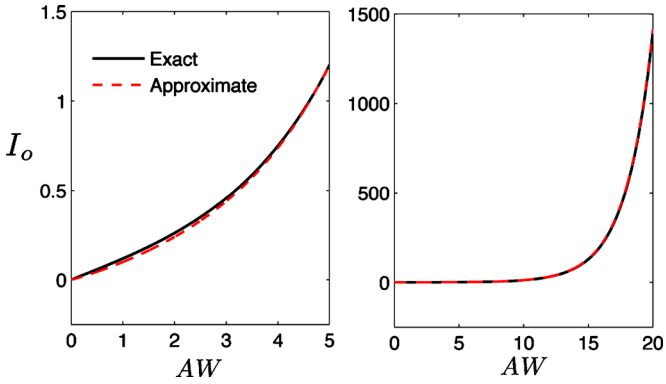

FIG. 8. (Color online) The approximation of the integral I_o, from Eq. (B22) (red dashed line) accurately represents the exact result calculated numerically (black line).

$$\int_0^\infty dk_\perp \frac{k_\perp}{(k_\parallel^2 + k_\perp^2)^2} = \frac{1}{2k_\parallel^2}. \tag{B19}$$

Using the substitution $x \equiv k_\parallel \lambda_{De}/\sqrt{A}$, Eq. (B18) becomes $I = A^{5/2}\lambda_{De}^{-4} I_o/2$, where

$$I_o \equiv \int_{-1}^{1} dx x^3 \sqrt{1-x^2}\exp(WAx\sqrt{1-x^2}). \tag{B20}$$

This integral can be approximated by taking both the small argument expansion of the exponential and the asymptotic limit of the integral, then matching the results with a Padé approximation. For small $w=AW$, the small argument expansion yields $I_o = 4w/35 + \mathcal{O}(w^3)$. The asymptotic behavior of this integral for large w is $I_o \equiv 3/(10\sqrt{w})\exp(w/2)$. It is hard to match the 4/35 and 3/10 number precisely, but a choice that works well for all w is

$$I_o \equiv \frac{3}{10}\frac{w\exp(w^2/2)}{4 + w^{3/2}}. \tag{B21}$$

Figure 8 shows that Eq. (B21) provides an excellent approximation for this integral over a very broad range of $w=AW$. We will only be interested in $2 \gtrsim AW \gtrsim 10$ here.

Putting Eq. (B21) into Eq. (B17), an approximate expression for the instability-enhanced collisional friction is

$$\mathbf{R}_{\mathrm{IE}}^{1-2} \approx -\frac{3q_1^2 q_2^2 n_1 n_2}{10 m_{12} \bar{v}_T^2}\frac{A^{7/2}W}{4 + (AW)^{3/2}} \times \frac{\alpha^{5/2}\exp(AW/2)}{(1+\alpha)(1-\alpha^2)^2}\frac{\Delta V^4 \Delta \mathbf{V}}{c_s^4 \Delta V_{\mathrm{up}}}. \tag{B22}$$

[1] D. Bohm, in *The Characteristics of Electrical Discharges in Magnetic Fields*, edited by A. Guthrie and R. K. Wakerling (McGraw-Hill, New York, 1949), Chap. 3.
[2] K.-U. Riemann, Phys. Plasmas **4**, 4158 (1997).
[3] L. Oksuz and N. Hershkowitz, Phys. Rev. Lett. **89**, 145001 (2002).
[4] M. A. Lieberman and A. J. Lichtenberg, *Principles of Plasma Discharges and Materials Processing*, 2nd ed. (Wiley, Hoboken, NJ, 2005), p. 182.
[5] P. C. Stangeby, J. Phys. D **20**, 1472 (1987).
[6] A. Barjatya, C. M. Swenson, D. C. Thompson, and K. H. Wright, Jr., Rev. Sci. Instrum. **80**, 041301 (2009).
[7] R. F. Fernsler, Plasma Sources Sci. Technol. **18**, 014012 (2009).
[8] D. Tskhakaya, S. Kuhn, and Y. Tomita, Contrib. Plasma Phys. **46**, 649 (2006).
[9] K.-U. Riemann, IEEE Trans. Plasma Sci. **23**, 709 (1995).
[10] M. S. Benilov, J. Phys. D: Appl. Phys. **29**, 364 (1996).
[11] H.-B. Valentini and F. Herrmann, J. Phys. D **29**, 1175 (1996).
[12] K.-U. Riemann, J. Phys. D **36**, 2825 (2003).
[13] S. D. Baalrud and C. C. Hegna, "Kinetic theory of the presheath and the Bohm criterion," Plasma Sources Sci. Technol. (in press).
[14] R. N. Franklin, J. Phys. D **33**, 3186 (2000).
[15] R. N. Franklin, J. Phys. D **34**, 1959 (2001).
[16] R. N. Franklin, J. Phys. D **36**, 34 (2003).
[17] R. N. Franklin, J. Phys. D **36**, 1806 (2003).
[18] R. N. Franklin, J. Phys. D **36**, R309 (2003).
[19] G. D. Severn, X. Wang, E. Ko, and N. Hershkowitz, Phys. Rev. Lett. **90**, 145001 (2003).
[20] N. Hershkowitz, Phys. Plasmas **12**, 055502 (2005).
[21] N. Hershkowitz, E. Ko, X. Wang, and A. M. A. Hala, IEEE Trans. Plasma Sci. **33**, 631 (2005).
[22] G. D. Severn, X. Wang, E. Ko, N. Hershkowitz, M. M. Turner, and R. McWilliams, Thin Solid Films **506–507**, 674 (2006).
[23] D. Lee, G. Severn, L. Oksuz, and N. Hershkowitz, J. Phys. D **39**, 5230 (2006).
[24] D. Lee, N. Hershkowitz, and G. D. Severn, Appl. Phys. Lett. **91**, 041505 (2007).
[25] X. Wang and N. Hershkowitz, Phys. Plasmas **13**, 053503 (2006).
[26] L. Oksuz, D. Lee, and N. Hershkowitz, Plasma Sources Sci. Technol. **17**, 015012 (2008).
[27] D. Lee, L. Oksuz, and N. Hershkowitz, Phys. Rev. Lett. **99**, 155004 (2007).
[28] S. D. Baalrud, C. C. Hegna, and J. D. Callen, Phys. Rev. Lett. **103**, 205002 (2009).
[29] C.-S. Yip, N. Hershkowitz, and G. D. Severn, Phys. Rev. Lett. **104**, 225003 (2010).
[30] L. Landau, Phys. Z. Sowjetunion **10**, 154 (1936); *Collected Papers of L D Landau*, edited by D. ter Harr (Pergamon, London, 1965).
[31] A. Lenard, Ann. Phys. (N.Y.) **10**, 390 (1960).
[32] R. Balescu, Phys. Fluids **3**, 52 (1960).
[33] S. D. Baalrud, J. D. Callen, and C. C. Hegna, Phys. Plasmas **15**, 092111 (2008).
[34] S. D. Baalrud, J. D. Callen, and C. C. Hegna, Phys. Plasmas **17**, 055704 (2010).
[35] L. Spitzer and R. Harm, Phys. Rev. **89**, 977 (1953); R. S. Cohen, L. Spitzer, and P. M. Routly, *ibid.* **80**, 230 (1950).
[36] B. D. Fried and S. D. Conte, *The Plasma Dispersion Function* (Academic, New York, 1961).
[37] J. Vranjes, B. P. Pandey, M. Y. Tanaka, and S. Poedts, Phys. Plasmas **15**, 123505 (2008).
[38] C. Lin and M. Lin, Commun. Nonlinear Sci. Numer. Simul. **14**, 2597 (2009).
[39] I. A. Biloiu and E. E. Scime, Phys. Plasmas **17**, 113508 (2010); **17**, 113509 (2010).